Crazing Phenomena in PC/SAN Microlayer Composites

D. HADERSKI,[1] K. SUNG,[1] J. IM,[2] A. HILTNER,[1,*] and E. BAER[1]

[1]Department of Macromolecular Science and Center for Applied Polymer Research, Case Western Reserve University, Cleveland, Ohio 44106; [2]Dow Chemical Company, Midland, Michigan 48640

SYNOPSIS

The crazing behavior of coextruded microlayer sheets consisting of alternating layers of polycarbonate (PC) and styrene–acrylonitrile copolymer (SAN) was investigated as a function of PC and SAN layer thicknesses. In this study, the total sheet thickness remained essentially constant and the PC and SAN layer thicknesses were changed by varying both the total number of layers from 49 to 1857 and the PC/SAN volume ratio. Photographs of the deformation processes were obtained when microspecimens were deformed under an optical microscope. Three different types of crazing behavior were identified: single crazes randomly distributed in the SAN layers, doublets consisting of two aligned crazes in neighboring SAN layers, and craze arrays with many aligned crazes in neighboring SAN layers. The transition from single crazes to doublets was observed when the PC layer thickness was decreased to 6 microns. Craze array development was prevalent in composites with PC layer thickness less than 1.3 microns. It was concluded that SAN layer thickness was not a factor in formation of arrays and doublets; formation of craze doublets and craze arrays was dependent only upon PC layer thickness.

INTRODUCTION

Amorphous glassy polymers, such as polycarbonate (PC) and poly(styrene–acrylonitrile) (SAN), are excellent materials for use in many engineering applications. Numerous studies of amorphous glassy polymers have described the deformation processes, particularly crazing and shearbanding. The investigation of crazing mechanisms, including initiation and growth, has provided a greater understanding of the role of crazes in polymer toughness and fatigue resistance. Crazes in amorphous polymer sheets are load-bearing, cracklike defects with surfaces bridged by many 100 Å diameter microfibrils. The craze can grow indefinitely in length, following the minor principal stress trajectories. The craze also grows in width, although the craze opening is limited to between 0.5 and 1.0 μm.[1] Eventually, microfibril breakdown leads to formation of a crack and subsequent catastrophic fracture of the material.

The microdeformation mechanisms in coextruded PC/SAN microlayer composites have been studied by several authors.[2–6] Crazing in PC/SAN microlayer systems is confined to the brittle SAN layers. Stress concentration at the craze tip causes shear banding in the PC layer. During macroscopic fracture, drawing of the PC layers produces a damage zone ahead of the crack that diffuses stresses and retards crack propagation. When PC layers are thick, about 10–30 microns in size, no interaction between individual crazes in neighboring SAN layers is evident. However, studies of PC/SAN composites with up to as many as 776 layers show that when layer thickness decreases a transition from characteristic bulk behavior to synergistic effects takes place.

The aim of the present study was to characterize in detail the effect of layer thickness on the crazing behavior in PC/SAN microlayer composites. In particular, the effect of PC layer thickness on interactive crazing in neighboring SAN layers was examined. Qualitative results obtained by photographing microspecimens during tensile testing are presented in this article.

* To whom correspondence should be addressed.

Journal of Applied Polymer Science, Vol. 52, 121–133 (1994)
 CCC 0021-8995/94/020121-13

EXPERIMENTAL

Materials

A variety of microlayer composites was supplied by the Dow Chemical Co. in the form of coextruded sheets. The composites contained alternating layers of polycarbonate (PC) and styrene–acrylonitrile copolymer (SAN) with the outermost layers composed of PC.[7,8] The PC/SAN microlayer composites under investigation are shown in Table I. The PC and SAN layer thicknesses were changed by varying the total number of layers, ranging from 49 to 1857, along with the PC/SAN volume ratio. For this study, the materials are described by the layer thicknesses rather than by the number of layers or PC/SAN volume ratio. The average layer thickness was measured from optical and scanning electron micrographs.

Methods

The specimens for optical microscopy were prepared by cutting along the edge of a coextruded microlayer sheet with a diamond blade. This resulted in a rectangular specimen between 1.1 and 1.4 mm thick. The cut specimens were polished on a metallurgical wheel initially using fine sandpaper and, then, an aluminum oxide suspension. The central part of the specimen was thinned to between 0.4 and 0.6 mm to confine the deformation to this region. The polished specimen was clamped in place in a Polymer Laboratories Minimat microtensile tester for uniaxial tensile loading. The microtensile tester was mounted on the stage of an Olympus BH2 optical microscope so that the deformation processes could be photographed as the specimen was deformed. Unless otherwise specified, specimens were stretched at a speed of 0.01 mm per min.

Scanning electron microscopy was used to observe the surface of the deformed composite. The deformed microspecimen was mounted on a modified SEM tensile stage and stretched slightly to reopen the crazes. The specimen was then coated with a 30 Å layer of gold and observed under a low-voltage scanning electron microscope (JEOL, JSM-840A).

RESULTS AND DISCUSSION

Microdeformation Mechanisms

A representative stress–strain curve for the 49-layer PC/SAN (29/16 μm) composite microspecimen is shown in Figure 1. The composite deformed in a ductile manner and attained a yield stress of 62.5 MPa. The value of the yield stress was the same as that measured previously for macrotensile specimens of this composite.[2,3] The yield stress was between that of PC (62 MPa) and SAN (82 MPa)

Table I Layer Thickness and Composition of PC/SAN Microlayer Composites

No. Layers	PC/SCAN Vol Ratio[a]	Total Sample Thickness (mm)	Av PC Layer Thickness (μm)	Av SAN Layer Thickness (μm)
49	65/35	1.14	29.2	15.7
	62/38	1.08	27.1	16.6
	46/54	1.21	23.1	27.2
	28/72	1.15	12.8	32.9
194	76/24	1.12	10.3	3.3
	60/40	1.12	7.5	5.2
	43/57	1.28	5.9	7.9
	32/68	1.40	4.4	9.3
388	53/47	1.16	3.6	3.3
776	67/33	1.10	1.9	1.0
	55/45	1.10	1.5	1.2
	40/60	1.23	1.3	2.0
927	68/32	1.44	1.6	0.8
	36/64	1.37	0.8	1.6
1857	57/43	1.40	0.7	0.6
	31/69	1.38	0.4	1.0

[a] Calculated from measured layer thicknesses.

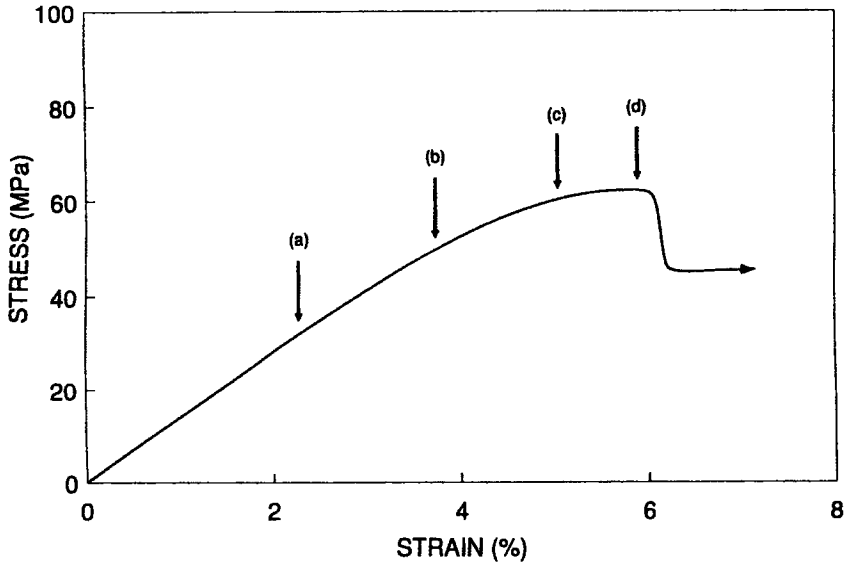

Figure 1 Typical stress–strain curve for 49-layer PC/SAN (29/16 μm) composite. Points (a)–(d) indicate strains at which optical micrographs in Figure 2 were obtained.

and obeyed the rule of mixtures. The primary difference between the stress–strain curves obtained in this study with microspecimens and previous studies that used macrospecimens was the postyield behavior. Due to the slow strain rate and thin gauge section, all the microspecimens were ductile and formed a stable neck.

The microdeformation behavior of PC/SAN microlayer composites was previously described,[2,3] but without relating the deformation events directly to the stress–strain curve. Optical microscopy revealed the formation of crazes oriented perpendicular to the stress direction. As evident in Figure 2(a) and (b), the first observable event was random crazing throughout the SAN layers. Crazing consisted only of single crazes, which were defined as crazes randomly distributed throughout the SAN layers with no regularity or registry between crazes in neighboring SAN layers. As strain increased to about 5% [Fig. 2(c)], more crazes formed, increasing the overall craze density in the specimen. In addition, localized shear deformation appeared in the PC layers initiated at the craze tips. The micro-shearbands extended partway into the PC layers [Fig. 2(d)]. At the yield strain, the micro-shearbands joined together across the entire PC layer as the SAN layers fractured.

Due to composite processing, the PC layers, and to a lesser extent the SAN layers, were considerably thinner near the specimen edge, especially in the 49-layer composite. When the PC layer thickness was small enough, craze doublets formed, i.e., a second craze formed in registry with an existing craze in a neighboring SAN layer. For example, in the 49-layer PC/SAN (13/33 μm) composite, the PC layer thickness near the specimen edge decreased to approximately 4 microns (Fig. 3). After some initial crazes formed in SAN layers near the specimen edge, another craze occasionally appeared in an adjacent SAN layer above or below an initial craze. A view of this region after deformation (Fig. 3) reveals several craze doublets composed of usually two but sometimes three vertically aligned crazes in neighboring SAN layers. Because deformation behavior near the edge was not necessarily representative of the composite, all microscopic observations were confined to the center region of the specimen where the layers were of uniform thickness.

Since the PC/SAN (29/16 μm) composite showed craze doublet formation only at the specimen edge where the PC layers were thinner, composites with thinner layers were examined. Craze doublets were observed in the 194-layer PC/SAN (5.9/7.9 μm) composite. A typical stress–strain curve for 194-layer PC/SAN (5.9/7.9 μm) is represented by Figure 4. The yield stress of 73.6 MPa was comparable to that previously obtained for macrospecimens under tensile testing. The yield stress was previously found to depend on composition, but not on the number of layers.[3] The yield stress of the 194-layer composite in Figure 4 was higher than that of the 49-layer composite in Figure 1 because the SAN content was 1.5 times higher. The yield strain, 5.5%, was the same as that of the 49-layer composite.

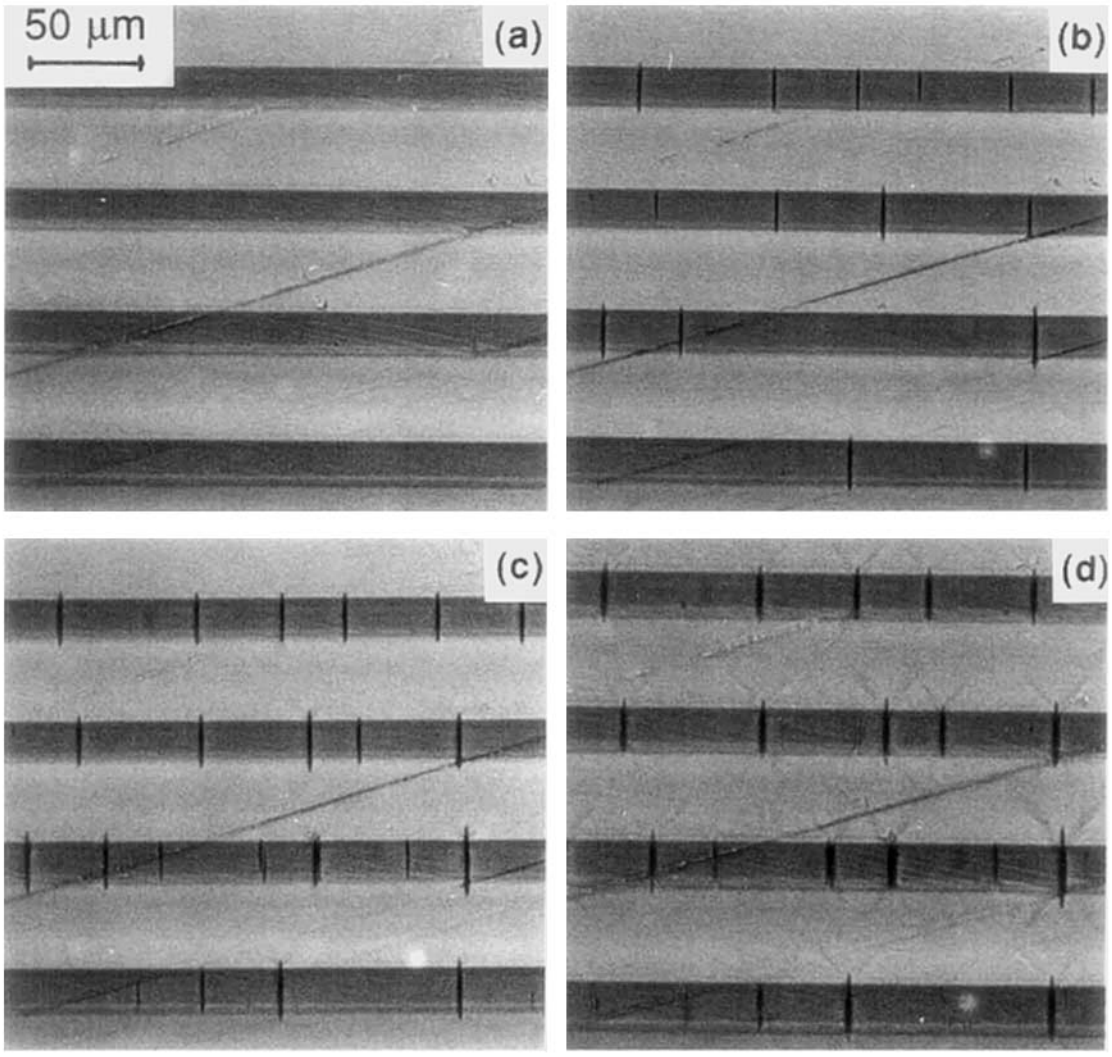

Figure 2 Optical micrographs of PC/SAN (29/16 μm) microlayer composite showing development of crazes and micro-shearbands with increasing strain: (a)–(d).

The optical micrographs in Figure 5 correspond to points (a)–(d) marked on the stress–strain curve. Initial crazing took place at about 2.0% strain, position (a), at the end of the linear portion of the curve, similar to the 49-layer composite. As seen in Figure 5(a), the initial deformation event was random crazing throughout the SAN layers, similar to the 49-layer sample. However, as strain increased, occasional craze doublets formed [Fig. 5(b)], along with more single crazes. Infrequently, a triplet appeared. The formation of doublets and growth of doublets to triplets was halted when micro-shearbands appeared at the craze tips [Fig. 5(c)]. The micro-shearbands coalesced just before yielding [Fig. 5(d)] and extended across the PC layers while some propagated through both the PC and SAN layers.

A representative stress–strain curve of the PC/SAN (0.8/1.6 μm) composite is shown in Figure 6. The yield stress, 78.5 MPa, was slightly higher than that of the 194-layer composite, which was consistent with the composition. An important difference was the longer linear region in the stress–strain curve of the 927-layer composite. Craze initiation coincided with the linear limit of the stress–strain curve in all the composites. Since craze initiation occurred at a higher strain in the 927-layer composite, 3.3%, in contrast to 2.0% for the 49- and 194-layer composites, the linear portion of the curve was longer.

Initial crazing was random throughout the SAN layers of the 927-layer PC/SAN (0.8/1.6 μm) composite [Fig. 7(a)]. However, very rapidly, additional

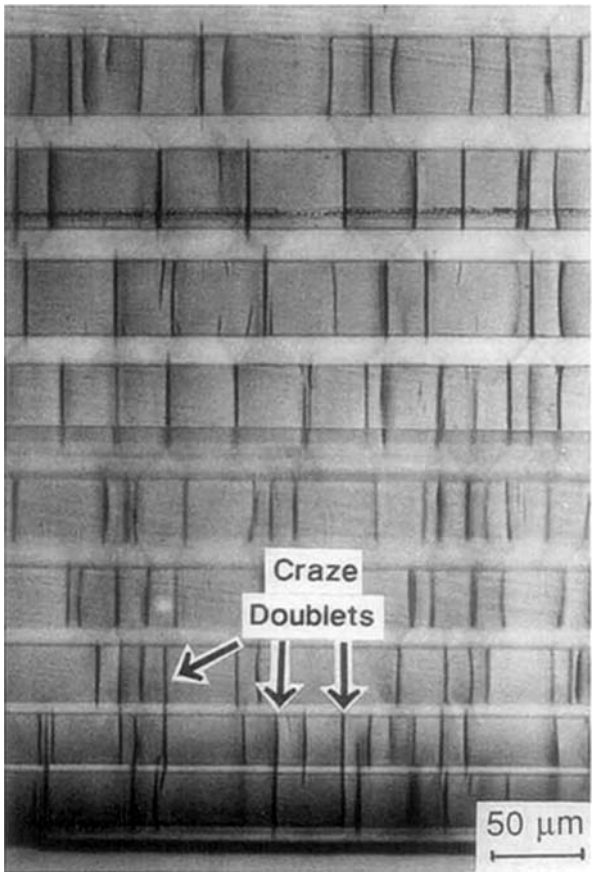

Figure 3 Specimen edge region of 49-layer PC/SAN (13/33 μm) composite showing decreasing PC layer thickness with subsequent craze registration in neighboring SAN layers.

crazes formed in registry in the neighboring SAN layers, resulting in craze arrays [Fig. 7(b) and (c)]. Propagating rapidly from one SAN layer to the next, the craze arrays grew to comprise many SAN layers. This phenomenon was unlike the craze doublets, which involved only two SAN layers. Furthermore, craze doublets made up a small fraction of the total crazes, whereas craze arrays consumed almost all the crazes in the specimen.

Craze array growth was terminated by the formation of micro-shearbands at the craze tips [Fig. 7(c)], as was the case for craze doublets and single crazes. Micro-shearbands that initiated in the PC layers propagated through both PC and SAN layers [Fig. 7(d)]. Close to yielding [Fig. 7(e)], the micro-shearbands thickened and coalesced into a network that eventually produced global yielding of both PC and SAN layers. The micro-shearbands that grew from the craze tips were approximately the same length in all the composites. The important feature was the relationship of the micro-shearband length to the layer thickness. When the layers were thin, a micro-shearband could extend through many alternating PC and SAN layers. A micro-shearband of the same length in a composite with thicker layers might not even have spanned a single PC layer.

Generally, a craze array formed from a single craze when additional crazes appeared in neighboring SAN layers in a line perpendicular to the stress direction. It was possible for the craze array to grow in either direction from the initial craze, and, frequently, it grew in both directions. The growth was

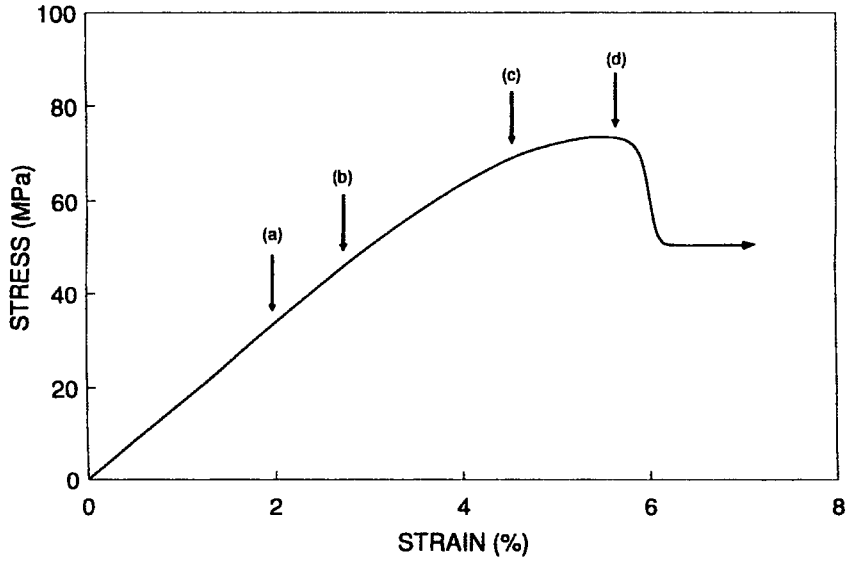

Figure 4 Typical stress–strain curve for 194-layer PC/SAN (5.9/7.9 μm) composite. Points (a)–(d) correspond to optical micrographs in Figure 5.

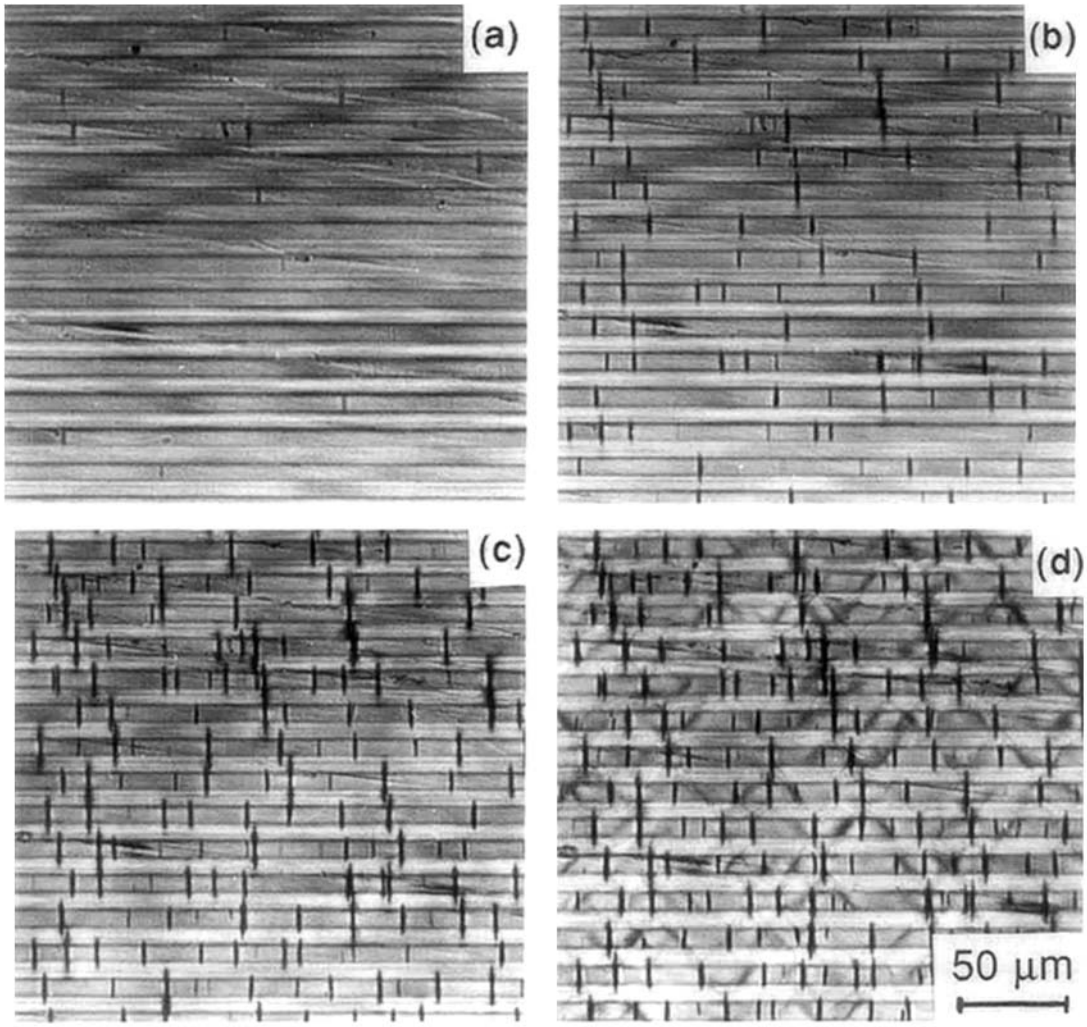

Figure 5 Optical micrographs of PC/SAN (5.9/7.9 μm) microlayer composite showing development of crazes, craze doublets, and micro-shearbands with increasing strain: (a)–(d).

quite rapid and stopped abruptly with micro-shearband formation at the craze tips. For example, the growth of two individual craze arrays in the PC/SAN (0.8/1.6 μm) composite is plotted in Figure 8. Initial craze formation occurred at 3.3% strain and craze arrays grew rapidly as strain increased. Array growth stopped at about 4.5% strain, when micro-shearbands appeared at the craze tips. With further increase in strain, the length of the craze arrays remained constant, as evident from the plateau on the curve in Figure 8.

Scanning electron microscopy of a deformed PC/SAN (0.8/1.6 μm) 927-layer composite specimen revealed the morphology of a craze array (Fig. 9). The craze array was composed of aligned single crazes in the SAN layers separated by plastically deformed PC layers. No delamination between the SAN and PC layers was evident, indicating good interlayer adhesion.

Layer Thickness

The relationship between crazing and layer thickness was examined by comparing the three types of crazing behavior. Three composites that represented the different types of behavior were used to develop the schematic diagram in Figure 10. The 49-layer PC/SAN (29/16 μm) composite contained only

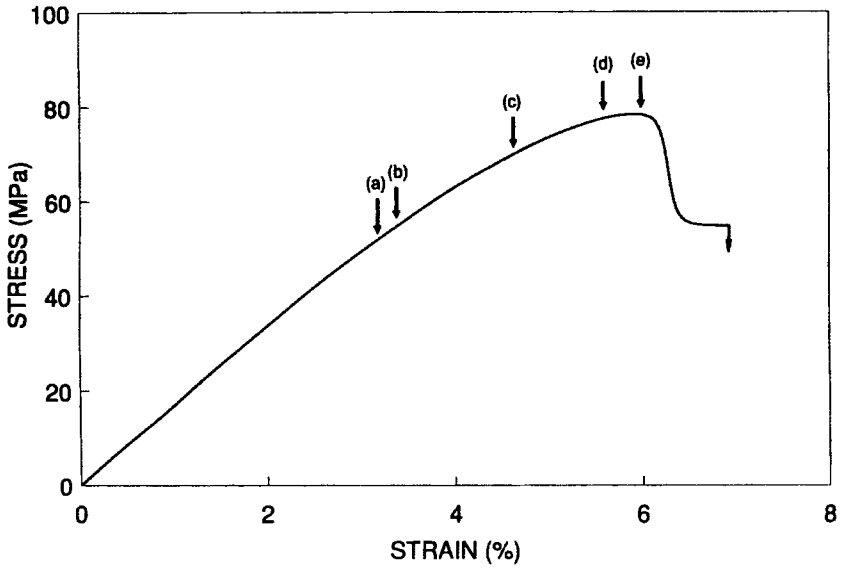

Figure 6 Typical stress–strain curve for 927-layer PC/SAN (0.8/1.6 μm) composite. Points (a)–(e) on the curve represent strains at which optical micrographs in Figure 7 were obtained.

random single crazes in the SAN layers. The crazes usually initiated at the PC/SAN interface and grew slowly across the SAN layer. In the 194-layer PC/SAN (5.9/7.9 μm) composite, most of the crazes were randomly distributed single crazes, although 20–30% of the crazes were in craze doublets. The diagram shows that crazing initiated in the 927-layer PC/SAN (0.8/1.6 μm) composite at a higher strain, 3.3%, than in the other two composites. The type of crazing in the 927-layer composite was also quite different. Almost immediately after crazing initiated, craze arrays began to propagate rapidly through many layers.

The crazing behavior of 16 compositions of varying layer thickness and PC/SAN volume ratio was examined. The composites were categorized by whether crazing occurred as single crazes, craze doublets, or craze arrays, and the relationship of crazing type to PC and SAN layer thickness is presented as a map in Figure 11. A correlation was observed with the PC layer thickness, but not with the SAN layer thickness. Only random crazing was observed when the PC layer thickness was greater than 6 microns. Craze doublets were observed in composites with PC layer thickness less than or equal to 6 microns, but greater than 1.3 microns. The composite with 1.3 micron PC layer thickness was transitional and showed craze doublets, craze triplets, and short craze arrays involving four or five SAN layers. A PC layer thickness of less than 1.3 microns produced craze arrays. It should be emphasized that craze array formation did not depend on SAN layer thickness, but depended on the thickness of PC layers. For example, a composite with a SAN layer thickness of 3.3 microns formed only random single crazes with a PC layer thickness of 10.3 microns (194 layers, PC/SAN (10.3/3.3 μm), but exhibited craze doublet formation when the PC layer thickness was 3.6 microns (388 layers, PC/SAN (3.6/3.3 μm).

In all cases, growth of craze doublets and craze arrays ceased with formation of micro-shearbands at the craze tips. In the 49-layer PC/SAN (29/16 μm) composite, the shearbands extended only part way through the PC layers. Only when the yield strain was approached did the shearbands coalesce and span the entire PC layer. During yielding, the crazes in the SAN layers opened up into cracks or voids and the shearbanding produced drawing of the PC layers. For the 194-layer PC/SAN (5.9/7.9 μm) composite, the micro-shearbands extended through the PC layers and joined just prior to necking, sometimes propagating through the PC layer into the next SAN layer. Again, the SAN layers fractured during necking. The micro-shearbands in the 927-layer PC/SAN (0.8/1.6 μm) composite coalesced and extended through many PC and SAN layers. When this composite yielded, the SAN layers were

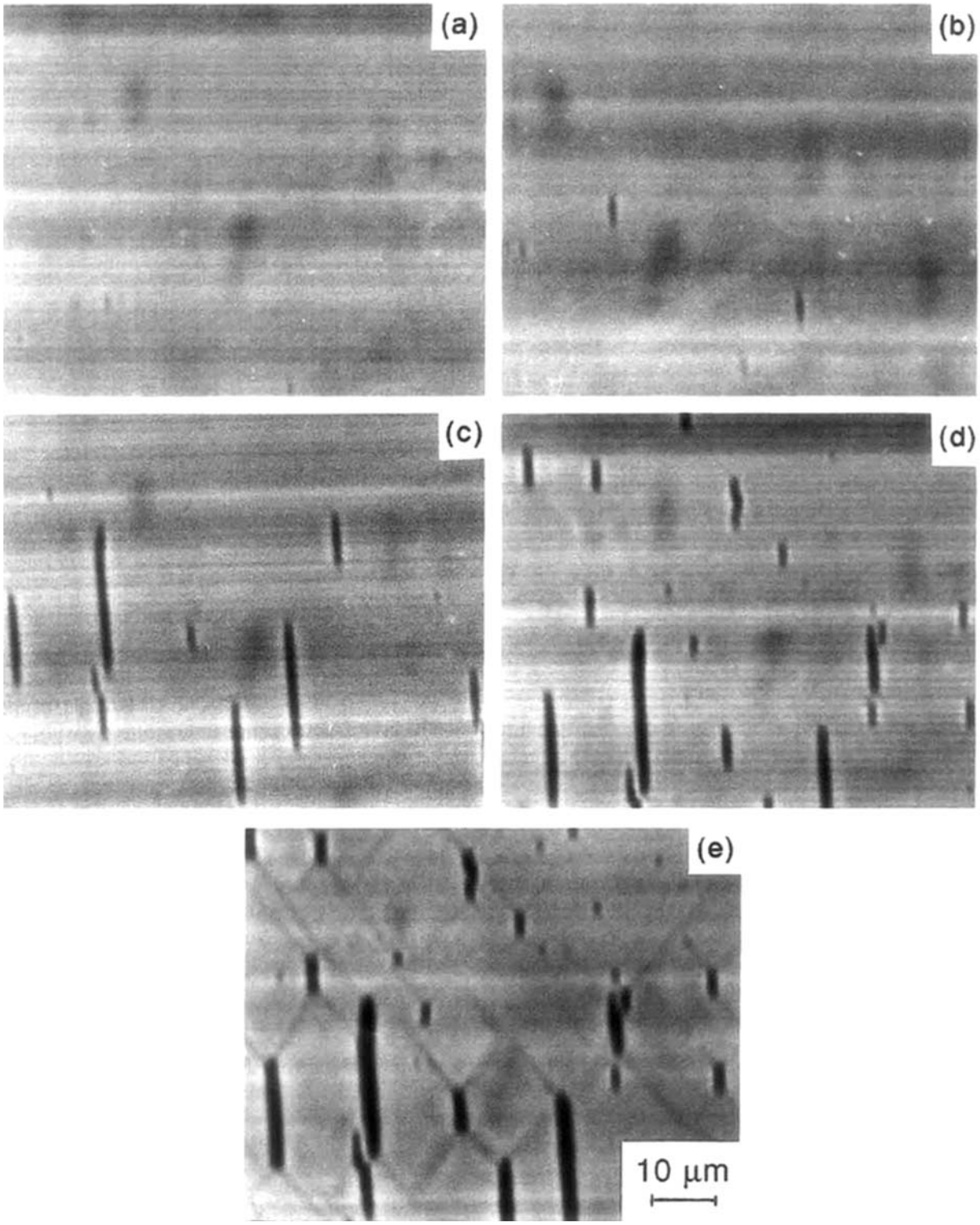

Figure 7 Optical micrographs showing development of crazes, craze arrays, and microshearbands in PC/SAN (0.8/1.6 μm) microlayer composite as a result of increasing strain: (a)–(e).

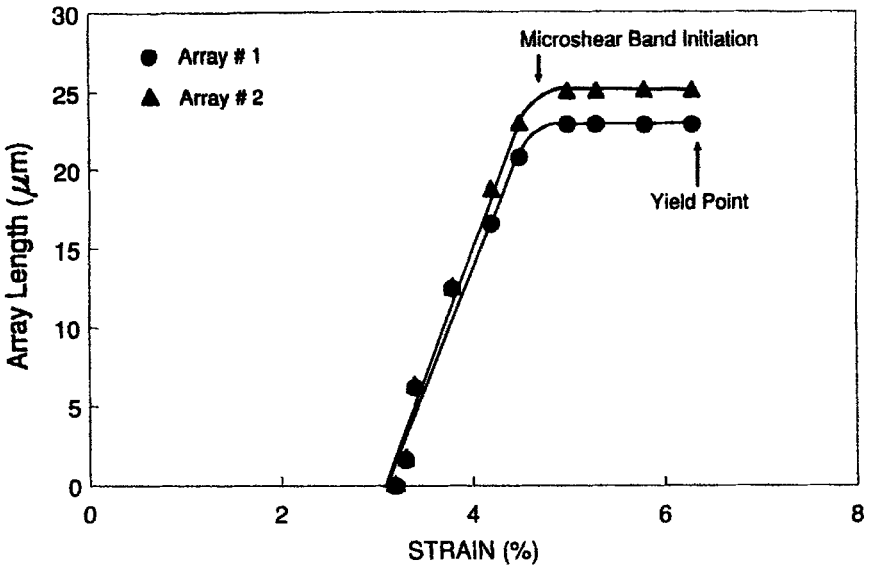

Figure 8 Craze array growth as a function of strain for two individual craze arrays formed in 927-layer PC/SAN (0.8/1.6 μm) composite.

drawn along with the PC layers as the entire composite necked. This was different from the other two composites where only the PC layers were drawn while the SAN layers fractured and voided.

Craze Density

The number of single crazes, craze doublets, and craze arrays varied widely through the range of layer

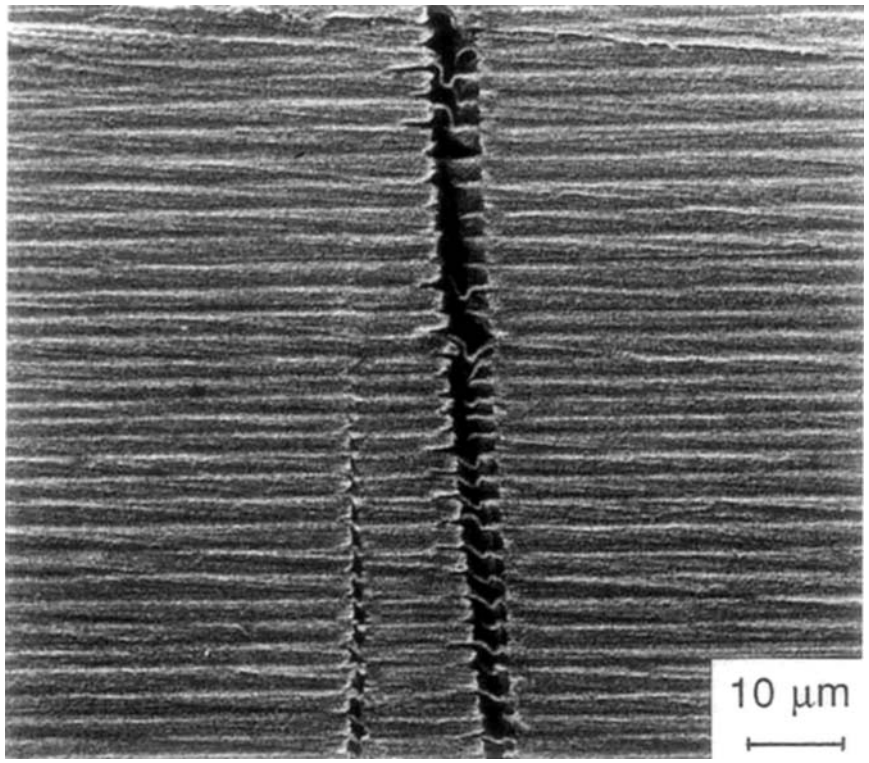

Figure 9 Scanning electron micrograph showing a typical craze array structure.

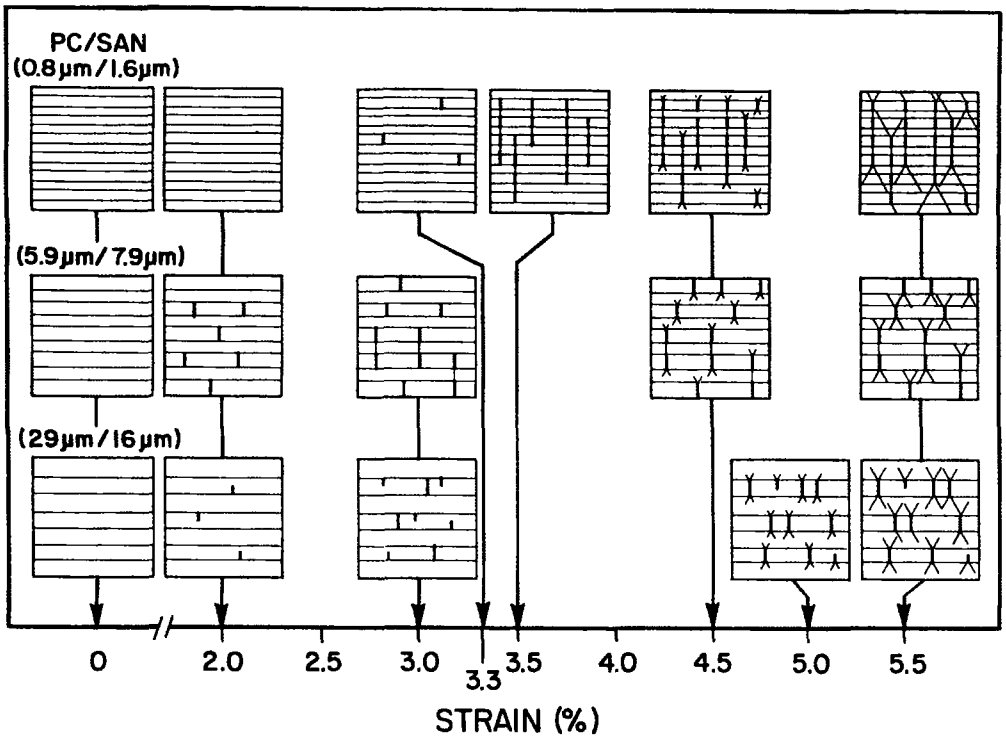

Figure 10 Schematic comparison of crazing and micro-shearbanding in PC/SAN microlayer composites.

thicknesses. The craze density was studied for three representative cases: 49-layer PC/SAN (26/16 μm) composite, 194-layer PC/SAN (5.9/7.9 μm) composite, and 927-layer PC/SAN (0.8/1.6 μm) composite. This was accomplished by counting the number of single crazes, craze doublets, and craze arrays and the number of crazes in each craze array in the optical micrographs. The total number of crazes increased as the number of layers increased, and a convenient way to normalize the results for different compositions was to present the linear craze density, defined as the number of crazes per unit length of SAN layer. The resulting plots of linear craze density as a function of strain for the three

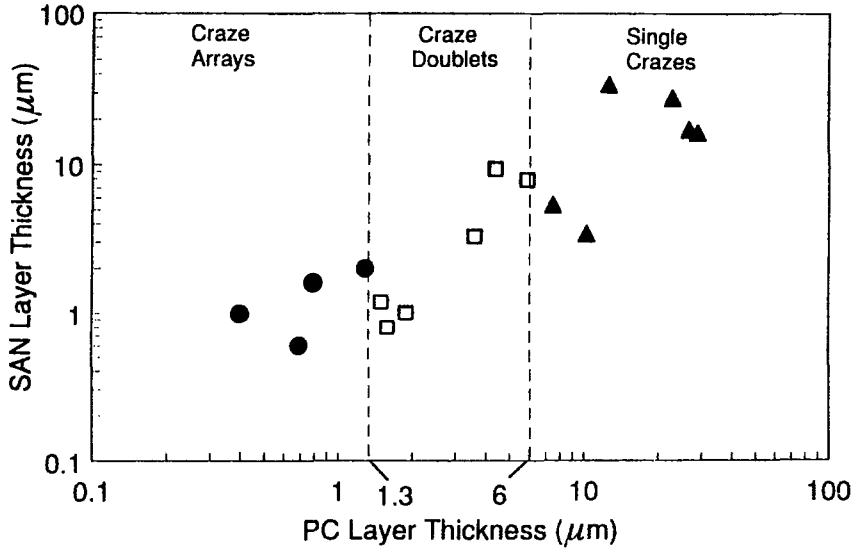

Figure 11 Type of crazing as a function of PC and SAN layer thicknesses.

composites are shown in Figure 12. For PC/SAN (29/16 μm) composite [Fig. 12(a)], only single crazes were observed. For the PC/SAN (5.9/7.9 μm) composite, crazing consisted of single crazes and craze doublets with single crazes dominating. It is evident from Figure 12(b) that the number of single crazes was very close to the total number of crazes. In the PC/SAN (0.8/1.6 μm) composite, the number of single crazes was very low, indicating that most of the crazes were part of a craze array [Fig. 12(c)].

The percent of total crazes in craze arrays as a function of PC layer thickness is depicted in Figure 13. When the PC layer thickness was greater than 6 microns, there were no craze doublets or arrays, only single crazes. When the PC layer thickness was decreased into the 1.5–6 micron range, most of the crazes formed were single crazes, but about 20% were in craze doublets. When the PC layer thickness reached 1.3 microns, there was a transition from single crazes with some craze doublets to craze arrays. When the PC layer thickness was less than 1.3 microns, virtually all the crazes were in craze arrays. At a PC layer thickness of 1.3 microns, there was a transition from predominately single crazes with some craze doublets to mostly craze arrays.

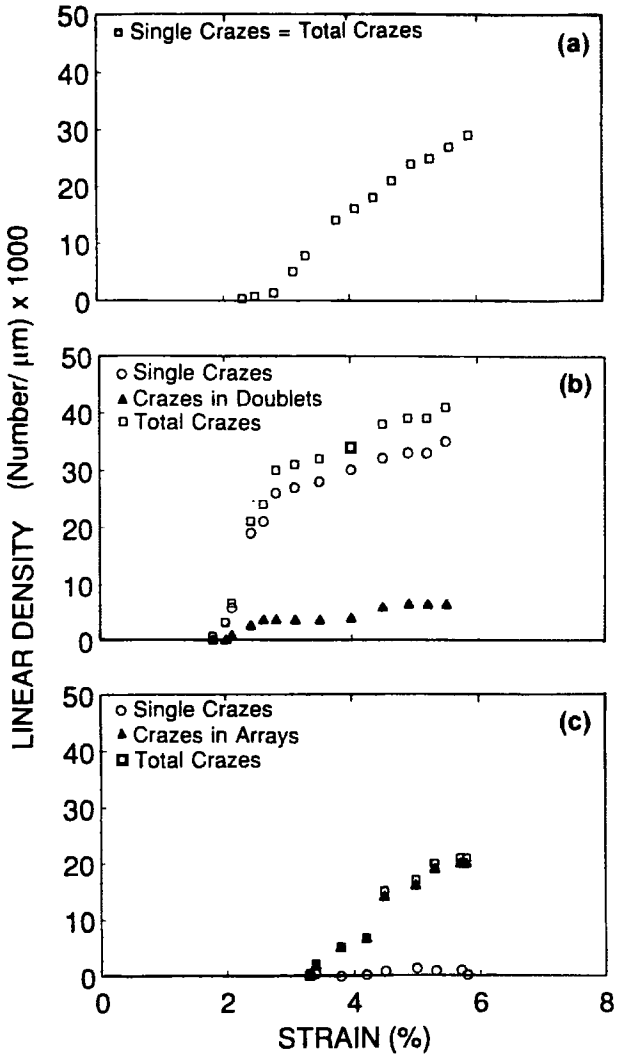

Figure 12 Linear craze density as a function of strain for (a) 49-layer PC/SAN (29/16 μm) composite, (b) 194-layer PC/SAN (5.9/7.9 μm) composite, and (c) 927-layer (0.8/1.6 μm) composite.

The average number of SAN layers in a craze doublet or array is summarized for the different PC layer thicknesses in Figure 14. Single crazes were not counted. In specimens with a PC layer thickness in the range of 1.3–6 microns, the average number of SAN layers in an array was two, indicating craze doublets. When the PC layer thickness decreased below 1.3 microns, the average number of SAN layers involved increased.

Growth of craze doublets and craze arrays from a single craze occurred slowly enough to be easily followed in the optical microscope as the composite was stretched. Taken together with the well-known strain rate sensitivity of crazing in general, this suggested that the transitions from craze arrays to craze doublets to single crazes in Figures 13 and 14 would be affected by strain rate. This dependency was examined with the 776-layer PC/SAN (1.3/2.0 μm) composite. At the low testing speeds, 0.01–1.0 mm/min, this composite was ductile; yielding was followed by stable neck propagation and fracture at a strain of about 100%. Higher test speeds resulted in a decreased fracture strain. A neck formed but did not propagate in a stable manner at test speeds of 5.0 and 10.0 mm/min, whereas at the highest test speed, 20.0 mm/min, the composite fractured without yielding. The craze density was about the same at all test speeds except 20.0 mm/min, where only a few single crazes formed before the composite fractured.

At the lowest test speed, 0.01 mm/min, the crazing behavior of this composite was transitional with about 55% of the crazes in craze arrays. The effect of test speed on the fraction of crazes in arrays, triplets, and doublets and as single crazes is summarized in Table II. As the test speed increased, the type of crazing shifted from predominantly craze arrays to a larger fraction of craze doublets and, finally, to virtually only single crazes. A transition from craze arrays to craze doublets occurred when the test speed was increased from 0.01 to 0.05 mm/min. The disappearance of craze arrays and the concurrent increase in the fraction of craze doublets from 9 to

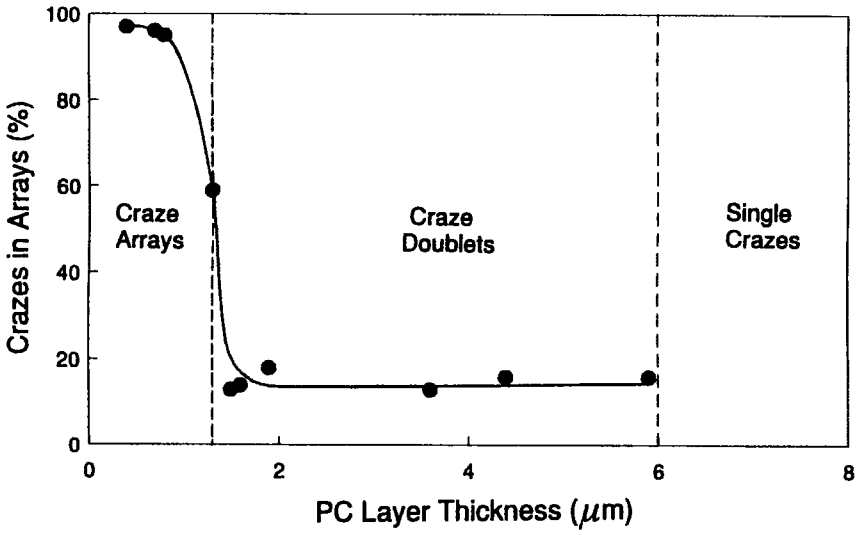

Figure 13 Percent of total crazes in a craze array vs. PC layer thickness.

22% and in the fraction of single crazes from 19 to 67% were very distinct. At a test speed of 0.05 mm/min, the fraction of crazes in triplets and doublets in the 776-layer PC/SAN (1.3/2.0 μm) composite was comparable with other compositions that were characterized as forming craze doublets. A subsequent transition from craze doublets to single crazes took place as the test speed was increased to 0.5 mm/min. At this test speed, essentially only single crazes formed. There was no other change in the crazing behavior as the test speed was increased further, until at the highest speed, 20.0 mm/min, the composite fractured before crazing took place.

CONCLUSIONS

It was determined from this study of microdeformation behavior that crazing of SAN layers in PC/SAN microlayer composites exhibits the following features:

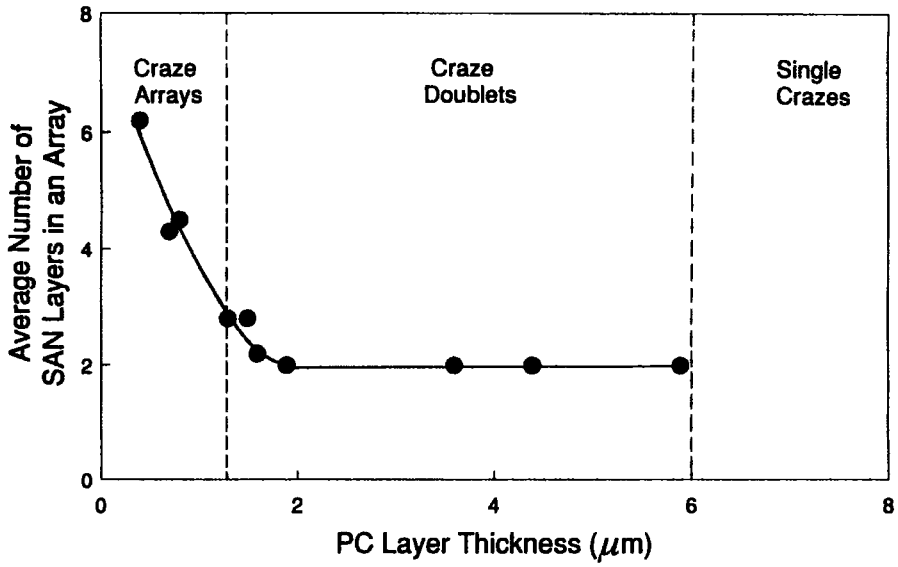

Figure 14 Average number of SAN layers in a craze array as a function of PC layer thickness.

Table II Effect of Test Speed on Crazing Phenomena of 776-Layer PC/SAN (1.3/2.0 μm) Composite

Test Speed (mm/min)	F_S (%)	F_D (%)	F_T (%)	F_A (%)	ϵ_F (%)
0.01	19	9	17	55	~ 100
0.05	67	22	11	0	~ 100
0.1	88	11	1	0	~ 100
0.5	97	3	0	0	~ 100
1.0	97	2	1	0	~ 100
5.0	98	2	0	0	14
10.0	100	0	0	0	9.7
20.0	100	0	0	0	5.3

F_S: fraction of single crazes; F_D: fraction of crazes in doublets; F_T: fraction of crazes in triplets; F_A: fraction of crazes in arrays; ϵ_F: fracture strain.

1. Craze initiation begins at a significantly higher strain in composites with thin layers, thus creating a longer than usual linear region on the stress–strain curve.
2. Crazing behavior depends only on the PC layer thickness, not on the thickness of SAN layers.
3. During deformation, only single crazes form in specimens with PC layer thickness greater than 6 microns. A PC layer thickness between 1.3 and 6 microns results in craze doublet formation, whereas a composite with PC layer thickness less than 1.3 microns gives rise to predominantly craze arrays.
4. Craze growth stops in all composites with formation of micro-shearbands at the craze tips.

The authors wish to thank the Dow Chemical Co., Midland, MI, for supplying the microlayer composites. For the continuing financial support, the authors thank the National Science Foundation, Polymers Program (9100300).

REFERENCES

1. E. J. Kramer and L. L. Berger, in *Advances in Polymer Science, 91/92, Crazing in Polymers,* Vol. 2. H.-H. Kausch, Ed., Springer-Verlag, Berlin, 1990, p. 1.
2. B. L. Gregory, A. Siegmann, J. Im, A. Hiltner, and E. Baer, *J. Mater. Sci.,* **22,** 532 (1987).
3. M. Ma, K. Vijayan, J. Im, A. Hiltner, and E. Baer, *J. Mater. Sci.,* **25,** 2039 (1990).
4. A. Hiltner, K. Sung, E. Shin, S. Bazhenov, J. Im, and E. Baer, *Mater. Res. Soc. Symp. Proc.,* **255,** 141 (1992).
5. E. Shin, A. Hiltner, and E. Baer, *J. Appl. Polym. Sci.,* **47,** 245 (1992).
6. E. Shin, A. Hiltner, and E. Baer, *J. Appl. Polym. Sci.,* **47,** 269 (1992).
7. W. J. Schrenk, U.S. Pat. 3,884,606 (1975).
8. W. J. Schrenk and T. Alfrey, Jr., in *Polymer Blends,* D. R. Paul and S. Newman, Ed., Academic Press, New York, 1978, Vol. 2, p. 129.

Received February 26, 1993
Accepted May 21, 1993